FEBS Letters 539 (2003) 14–18 FEBS 27059

Structural study of a single-point mutant of *Sulfolobus solfataricus* alcohol dehydrogenase with enhanced activity

Luciana Esposito[a], Ilaria Bruno[b], Filomena Sica[a,b], Carlo Antonio Raia[c], Antonietta Giordano[c], Mosè Rossi[c], Lelio Mazzarella[a,b], Adriana Zagari[a,d,*]

[a] *Istituto di Biostrutture e Bioimmagini, CNR, via Mezzocannone 6-8, I-80134 Napoli, Italy*
[b] *Dipartimento di Chimica, Università degli Studi di Napoli 'Federico II', via Cinthia, I-80126 Napoli, Italy*
[c] *Istituto di Biochimica delle Proteine, CNR, via Marconi 10, I-80125 Napoli, Italy*
[d] *Dipartimento di Chimica Biologica, Università degli Studi di Napoli 'Federico II', via Mezzocannone 6, I-80134 Napoli, Italy*

Received 8 January 2003; revised 7 February 2003; accepted 7 February 2003

First published online 5 March 2003

Edited by Hans Eklund

Abstract Alcohol dehydrogenase from *Sulfolobus solfataricus* (SsADH) is the only enzyme from Archaea among the structurally studied members of the medium-chain ADH family described so far. Here, we present the three-dimensional structure of the apo form of the mutant N249Y which exhibits increased catalytic activity when compared to the wild-type enzyme. The substitution, located in the coenzyme binding domain, decreases the affinity for NAD(H) cofactor. The rearrangement of segments 248–250 and 270–275, induced by the mutation, suggests an explanation for the lower coenzyme affinity. This study also highlights the role in SsADH catalysis of the flexible loops located at the interface between the catalytic and the coenzyme domains.

Key words: Crystal structure; Alcohol dehydrogenase; Single mutation; Enzyme activation; Coenzyme binding

1. Introduction

Alcohol dehydrogenases (ADHs) are spread throughout the three domains of life: Eukarya, Bacteria, and Archaea. *Sulfolobus solfataricus* ADH (SsADH) is the first archaeal enzyme from the medium-chain ADH family for which the 3D structure was described [1]. It is an NAD(H)-dependent oxidoreductase which shows broad substrate specificity, high thermostability, and thermophilicity [2]. Its tetrameric structure is a typical dimer of dimers. Each subunit is formed by two domains, a coenzyme binding domain adopting a Rossmann fold, and a catalytic domain with two zinc ions playing a catalytic and a structural role. The overall fold of a single SsADH monomer is very similar to that of mammalian and bacterial ADHs [3–5] with major differences observed in the architecture of the substrate pocket, in the size of the interdomain cleft, and in the coordination of both the active site and the structural zinc ions [1].

Prior to the structural determination, a random mutagenesis strategy was adopted in order to find SsADH mutants endowed with improved catalytic properties. The mutant N249Y, containing the substitution in the coenzyme binding domain, showed strikingly different properties when compared to the wild-type (wt) enzyme [6]. Indeed, the N249Y substitution increases by six-fold the turnover number measured at 65°C with benzyl alcohol as substrate. The turnover number for the reverse reaction is also increased, while the affinity for all substrates decreases. Furthermore, the affinity for coenzymes is substantially lower than that of the wt protein (Michaelis constant K_M for NAD^+, 25-fold greater; K_M for NADH, 16-fold greater; dissociation constant K_d for NAD^+ and for NADH, 10^3-fold greater) [6]. Hence, the substitution N249Y probably increases the rate of coenzyme dissociation, thereby providing a possible explanation for the increased turnover since the release of the coenzyme is rate limiting for catalysis [6].

While considerably affecting the kinetics of the enzyme, the substitution does not perturb the structural stability. Indeed, the mutant resistance to heat, denaturants, and proteases turned out to be similar or even better than the parent protein.

To evaluate the molecular basis for the change in catalytic properties, we carried out a crystallographic study of the mutant N249Y SsADH. Given its low affinity for coenzymes, only crystals of the apo form have been obtained so far. The apo structure was therefore used to model the interactions between NADH and the coenzyme domain. Here, we report two crystal structures of the mutant, their comparison with the native protein, and the implications for coenzyme binding and activity.

2. Materials and methods

2.1. Crystallization and data collection

The mutant of the SsADH enzyme, Asn249Tyr, was expressed and purified from *Escherichia coli* following the procedure described previously [6].

Two crystal forms for the N249Y mutant of SsADH enzyme were obtained at 22°C by the microbatch method. Crystals of form I were grown under the same conditions found for the wt enzyme [7] and diffracted up to 2.5 Å resolution. They belong to the tetragonal space group $I4_122$ with one subunit in the asymmetric unit (a.u.), being isomorphous with wt apo SsADH crystals. In an attempt to optimize conditions, various additives were added to the crystallization drop. A second, monoclinic form (form II) was produced in the presence of 25 mM of cobalt chloride. Using macroseeding techniques, large single

*Corresponding author. Fax: (39)-081-2536603.
E-mail address: zagari@chemistry.unina.it (A. Zagari).

Abbreviations: ADH, alcohol dehydrogenase; SsADH, *Sulfolobus solfataricus* ADH; HLADH, horse liver ADH; wt, wild-type; NCS, non-crystallographic symmetry

0014-5793/03/$22.00 © 2003 Published by Elsevier Science B.V. on behalf of the Federation of European Biochemical Societies.
doi:10.1016/S0014-5793(03)00173-X

crystals of form II were obtained, which belong to space group C2 with six subunits in the a.u. Form II crystals diffract to higher resolution, 1.94 Å, and also show a lower mosaicity (0.3°) compared to form I crystals (0.7°).

Crystals of both forms were transferred to a stabilizing solution containing 18% glycerol as cryoprotectant. X-ray data were then collected at 100 K using synchrotron sources. Data were processed and scaled using the DENZO/SCALEPACK package [8]. Data collection statistics are shown in Table 1.

2.2. Structure determination and refinement

2.2.1. Monoclinic form (crystal form II). The N249Y SsADH structure of the monoclinic form was solved first, by using the molecular replacement program AMoRe [9]. The crystallographic structure of the wt protein, missing the loop 246–250 which embodies the mutation, was used as the search model. The rigid body refined solution resulted in six subunits in the a.u., corresponding to a correlation coefficient and an R factor of 54.8% and 38.2%, respectively. Four out of six chains form one tetramer and the remaining two chains belong to a second tetramer which is generated by the two-fold crystallographic axis.

The refinement was performed using the program CNS [10] omitting 5% reflections for the calculation of R_{free}. At the initial stages of refinement, strict non-crystallographic restraints were applied to the backbone and side chain atoms. Then the weights for the non-crystallographic symmetry (NCS) restraints were relaxed on the basis of the analysis of the R_{free} values over multiple refinement runs in which the NCS weights were varied.

Cycles of refinement were alternated with model building using $2F_{obs}-F_{calc}$ and $F_{obs}-F_{calc}$ electron density maps visualized by the program O [11]. The final model (model II) shows R and R_{free} factors of 21.0% and 24.4%, respectively, calculated by using data between 15 and 1.94 Å.

2.2.2. Tetragonal form (crystal form I). The crystal form is isomorphous to the wt SsADH crystal form already solved. The mutant structure was solved in a straightforward manner by using the molecular replacement program AMoRe and the single chain A from mutant form II as search model. Rigid body refinement of the initial molecular replacement solution gave a correlation coefficient of 76.8% and an R factor of 33.2% for data to 3.0 Å resolution. Further refinement was carried out using the program CNS, extending the resolution to 2.5 Å. A total of 8% of the reflections was used for R_{free} calculations. The final model accounts for all 347 residues, 120 water molecules, and two zinc ions resulting in R and R_{free} factors of 19.6% and 23.6%, respectively.

The stereochemistry of both crystalline models was validated with the program PROCHECK [12]. Refinement statistics are shown in Table 1. The coordinates of N249Y SsADH have been deposited at the Protein Data Bank with the codes 1NTO, 1NVG for the monoclinic and the tetragonal forms, respectively.

3. Results and discussion

3.1. The overall structure

Two crystal forms, a monoclinic and a tetragonal one, were obtained for the mutant enzyme. The tetragonal crystals are isomorphous to the wt crystals and contain one subunit in the a.u. (model I). The monoclinic crystal structure (model II) includes six independent monomers in the a.u. This provides the opportunity to compare the structure of the parent enzyme with that of its mutant, minimizing the bias that can be derived by different packings in the unit cell. Since model II was determined to the best resolution, it will serve as the reference model in this discussion.

Final model II was refined to 1.94 Å resolution. Chain A is the best ordered out of the six chains. Using subunit A as reference, the average rms deviation over all C^{α} atoms between this subunit and each of the remaining five ones is 0.31 Å. The largest differences in the backbone conformation are observed between chain A and chain C (rmsd = 0.43 Å). They reflect rigid body displacements of individual structural elements due to different packing environments. The rmsd between model II (chain A) and model I is also low (0.41 Å), thus indicating a substantially unaltered overall conformation in the two crystal forms. All subunits of the mutant structures show an interdomain cleft as wide as that found in the wt apo structure.

Model I and model II display poor electron density in the same regions, i.e. in the stretch 46–62 (see further discussion in Section 3.4) and at the N-terminal and C-terminal segments.

Table 1
Data collection and refinement statistics

	Crystal form I	Crystal form II
Data collection		
Synchrotron/beamline	ESRF-Grenoble/ID14-4	Elettra-Trieste
Space group	$I4_122$	C2
Cell constants (Å, °)	$a=b=125.40$, $c=117.19$	$a=215.33$, $b=91.59$, $c=118.24$, $\beta=99.2$
Resolution range (Å)	25–2.5 (2.59–2.5)[a]	15–1.94 (2.01–1.94)[a]
No. of measured/unique reflections	104 158/15 757	554 277/146 709
Completeness (%)	95.0 (96.9)	87.9 (86.9)
R_{merge} (%)[b]	3.6 (8.8)	3.3 (9.0)
$\langle I\rangle/\langle\sigma(I)\rangle$	33 (16)	30 (12)
No. of subunits/a.u.	1	6
Solvent content (%)	60	52
Refinement		
Resolution range (Å)	25–2.5	15–1.94
R (%)/R_{free} (%)[c]	19.6/23.6	21.0/24.4
No. of non-H protein atoms	2 620	15 709
No. of water molecules	120	633
No. of zinc ions	2	12
Rmsd from ideality		
Bonds (Å)	0.008	0.01
Angles (°)	1.3	1.5

[a] Statistics of the highest resolution shell are shown in parentheses.
[b] $R_{merge}=\Sigma_{\boldsymbol{h}}\Sigma_i|I_i(\boldsymbol{h})-\langle I(\boldsymbol{h})\rangle|/\Sigma_{\boldsymbol{h}}\Sigma_i|I_i(\boldsymbol{h})|$.
[c] R, $R_{free}=\Sigma_{\boldsymbol{h}}||F_{calc}(\boldsymbol{h})|-|F_{obs}(\boldsymbol{h})||/\Sigma_{\boldsymbol{h}}|F_{obs}(\boldsymbol{h})|$. The reflections used in the R_{free} calculation constituted 5% and 8% of the total number of reflections for the monoclinic and tetragonal crystal forms, respectively.

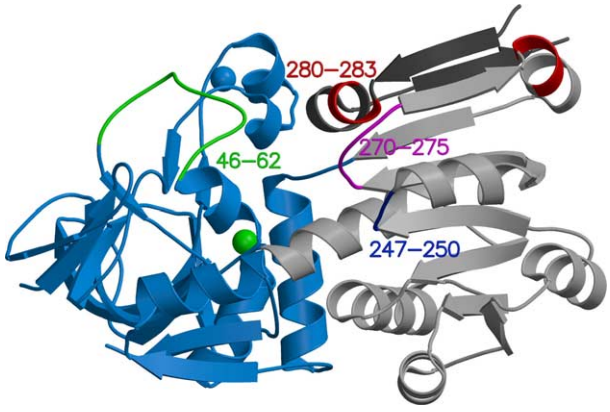

Fig. 1. Overall fold of the SsADH monomer (the catalytic and the coenzyme binding domains are shown in cyan and light gray, respectively). The segment 275–295 of another subunit forming a dimer (AB) is shown in dark gray. The catalytic and structural zinc ions are represented as green and cyan spheres, respectively. Regions of structural changes compared to the wt structure are highlighted in different colors (46–62 green, 247–250 blue, 270–275 magenta, 280–283 red).

3.2. Mutation site

The substitution N249Y in the coenzyme domain generates a structural rearrangement of residues 247–250 accompanied by an adjustment in the conformation of segment 270–275 (between βE and βS) and of segment 280–283, the N-terminal part of helix αF (Fig. 1).[1]

The structural changes necessary to accommodate a bulkier Tyr residue mainly involve the change in residue 248–249 conformations and the reorientation of the peptide plane O Val270–NGly271. Compared to the wt enzyme, the residue 249 side chain maintains its interaction with the loop 270–275 (Fig. 2A). In the mutant, a hydrogen bond is formed by the OH group of Tyr249 and the O of Phe273 (Fig. 2B), whereas in wt SsADH it is formed by the OD1 of Asn249 and the N of Gly271. The flipping of the plane 270–271 brings the main chain O of Val270 into H-bond contact with the N of Asn248 (Fig. 2A). This interaction establishes a different connection between the two adjacent loops which in the wt enzyme are connected by a hydrogen bond between O of residue 249 and N of Ala275 (Fig. 2B). Because of the different conformation of the 248–249 segment, the mutant enzyme also lacks the interactions between the Asp246 side chain and the peptide nitrogen atoms of residues 248 and 249.

Slight conformational changes at the 271–275 backbone between the two mutant structures are also observed. They are likely due to small variations at the AB dimer interfaces in the two crystal packings (Fig. 1) and they result in different optimized interactions between the side chain of the mutated residue and the 270–275 backbone. Indeed, in model II, the main chain O of Phe273 directly interacts with the OH group of Tyr249, whereas in model I an adjustment of the 271–275 backbone and a small rotation of the Tyr ring favor the H-bond between the phenolic OH and the O of Gly271.

The comparison of the mutant structure with the wt one indicates that loop 270–275 is rather flexible. A critical role for the structural rearrangement of this SsADH region seems to be played not only by Gly271, one of the most conserved residues in the ADH family, but also by Gly274 which adopts very different conformations in the SsADH structures, determined so far.

Interestingly, compared to the native structure, a notable movement close to the mutation also occurs at residue Phe273. In both wt and mutant structures, this is a particularly mobile residue which is exposed to the solvent displaying high B-factors. Nevertheless, in the wt structure the side chain is visible in its electron density and the same holds for at least one (chain A) out of six chains of model II, where a confident modeling could be made. The side chain was instead omitted from model I, due to the poor electron density that is barely visible beyond the CB atom. In model II the aromatic side chain lies on the surface and turns toward its own domain, whereas in the wt protein it points toward the catalytic domain forming a stacking interaction with the imidazole ring of His43 (Fig. 2B). The unfavorable solvent exposure of the hydrophobic Phe273 and its location in a loop which changes conformation in the coenzyme low-affinity mutant, suggest an implication of this residue in the binding of the cofactor.

Finally, a further noticeable change induced by the mutation is the small tilt of the N-terminal region (residues 280–283) of αF helix which shifts away from the adjacent loop 270–275 of the other subunit in the dimer (Fig. 1).

3.3. Implications for cofactor binding

To investigate the effect of N249Y substitution on coenzyme binding we model built the NADH molecule into its binding site by superposition with a ternary complex structure

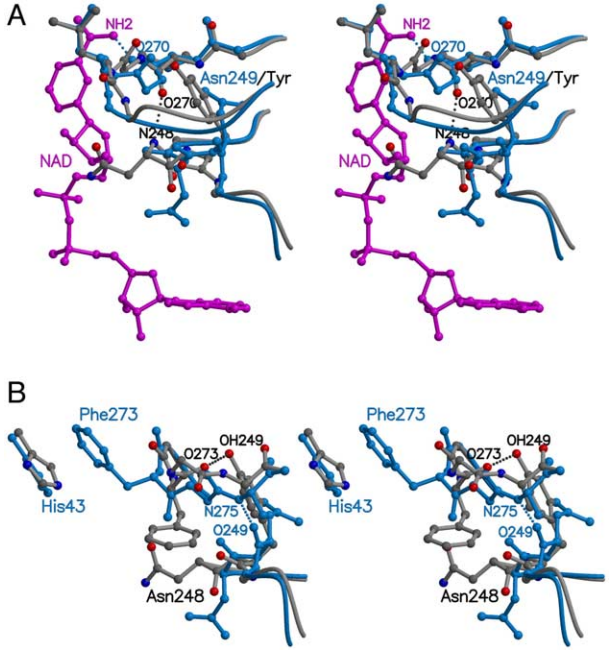

Fig. 2. Comparison of the regions 245–252 and 268–277 between the mutant (gray) and the wt (cyan) structures. A: The NADH molecule has been modeled by superimposing the HLADH holoenzyme complex (PDB code 2OHX) with the SsADH mutant. The coenzyme binding domains of the AB dimer have been used in the superposition. B: Interactions involving Phe273 and Asn249/Tyr (see Sections 3.2 and 3.3). Fig. 1 and this figure were drawn by the programs Molscript [21] and Raster3D [22].

[1] Here, we refer to the nomenclature of the secondary structural elements used in [1].

of the well-known horse liver ADH (HLADH) [13]. A core of structurally conserved residues from the coenzyme domain of SsADH and HLADH (see [1]) has been used in the superposition. The structural change in the mutated enzyme has two main consequences that can be relevant to cofactor binding at both the adenine and the nicotinamide sites.

Compared to the wt, the whole residue Asn248 is drawn toward the NADH binding cleft thus possibly interfering with a proper approach of the nicotinamide ribose to the Rossmann fold (Fig. 2A). Moreover, the displacement of Asn248 opens up the adenine binding pocket. Indeed in ADH structures the adenine ring is usually sandwiched between hydrophobic side chains. The alignment of SsADH with the other ADH structures shows that these two 'sandwich' positions are occupied by Val204 and by Asn248. Hence, the Asn248 displacement, due to the N249Y substitution, could produce packing deficiency that may well result in a poorer binding of the adenine moiety.

A second and perhaps more important effect is associated to the orientation of the peptide plane CO270–N271. The oxygen O270 does not point toward the NADH binding site, as observed in wt SsADH, but toward region 247–250 and it interacts with N of Asn248 (Fig. 2A). In most of the ADH holoenzyme structures the oxygen in this position acts as an anchoring point of the coenzyme by forming an H-bond to the NAD carboxamide amino group. In addition, this oxygen lies in a similar position in apo and holo HLADH structures. In mutant SsADH, the N271 is shifted to the equivalent position of the oxygen O270 as a result of the plane flipping. Hence, a possible stabilizing interaction (O–NH2) with the coenzyme in the wt structure, turns into an energetically unfavorable interaction between NH–NH2 groups in the mutant.

In conclusion, molecular modeling of the bound coenzyme suggests that the structural rearrangement induced by N249Y substitution would produce a less well-tailored binding site for the coenzyme. Although the mutant structure likely rearranges to relieve the steric conflicts and to tighten the binding of NAD carboxamide and adenine ring, this might be less efficient thus explaining the lower affinity for NAD(H).

It is worth noting that the mutation in SsADH causes substantial structural changes in loop 270–275, whose equivalent (292–298) in HLADH seems to be critical for the apo–holo conformational transition [3]. In fact, mutagenesis experiments performed on HLADH enzyme have shown that mutations in the flexible loop comprised of residues 292–298 affect the kinetics of the enzyme and especially coenzyme binding [14,15]. In both cases the affinity for the coenzyme decreases substantially. Crystallographic investigations of HLADH holoenzyme have shown that a conformational rearrangement of this segment is required for the 'closure' of the enzyme [3]. The movement of loop 292–298 provides space for the catalytic domain to come closer to the coenzyme binding domain.

It is still not clear what interactions in HLADH complexes are responsible for triggering the conformational change from the open to the closed form. However, several crystal structures of HLADH holo forms have pointed out that interactions with the nicotinamide ring are critical for the conformational change. In fact, the enzyme crystallized with ADP-ribose [16] or with coenzyme analogues [17,18] that are unable to establish interactions with the nicotinamide moiety, exhibits an open conformational state. The substitutions in the HLADH flexible loop, 292–298, were found to perturb the conformational equilibrium of the protein between the open and the closed form in the presence of the cofactor. An analogous crucial role can be suggested for loop 270–275 in SsADH given the hypothesis of similar conformational states for HLADH and SsADH enzymes.

3.4. Structural differences remote from the substitution site

A further noteworthy finding in the mutant structure concerns the disorder in loop 46–62 of the catalytic domain. This loop is located over the mouth of the active site just facing loop 270–275 on the other domain (Fig. 1). Region 46–62 shows high thermal factors and poor definition in electron density compared to the rest of the structure.

Loop 46–62 is one of the most flexible parts of the molecule in the wt structure too. However, the disorder appears to be more dramatic in the structures of the mutant, regardless of the different crystal packing environments.

Loop 46–62 is located on the interface between the two domains, and lies opposite the loop 270–275 which is likely to undergo a conformational transition upon cofactor binding. In HLADH the movement of the equivalent loops (51–58, 293–298) seems to be coupled. In fact, when NAD(H) binds, residues 293–298 of the coenzyme binding domain move away in order to make room for residues 51–58 from the catalytic domain which rotates to close the interdomain cleft [3].

At this interdomain interface in SsADH apo structures, van der Waals contacts are observed that involve residues Phe49, Asn51, Leu52, Leu272, Phe273, and Leu295. The rearrangement of loop 270–275 induced by the mutation may therefore be transmitted from one domain to the other, by altering the efficient clustering of these mostly hydrophobic side chains. As a result, the substitution can render the whole loop 46–62 more mobile and hence affect the flexibility of the active site in the mutant structure. In fact, loop 46–62 covers the active site and contributes to the hydrophobic channel which is the entrance for the substrate to access the catalytic zinc [3].

Finally, an increased flexibility of this loop region in the mutant structure could also be correlated to the different behavior shown by the mutated enzyme in the presence of mild denaturing conditions. In fact, low concentrations of sodium dodecyl sulfate (SDS) and guanidinium chloride increase the V_{max} for the wt enzyme (up to 115% by 0.05% SDS) while leaving the mutant V_{max} unaltered [6]. This is in line with what was observed for several other enzymes which exhibit an increased V_{max} and for which a correlation was suggested between the loosening of the active site structure and the enzyme activation by denaturants [19,20]. In this context, it may be surmised that diluted denaturants activate wt SsADH by inducing an increased flexibility at the active site, whereas the mutant is less sensitive to this effect due to its intrinsic loosening of the active site structure.

Acknowledgements: This work was supported by grants from ASI (Agenzia Spaziale Italiana) and CNR 'Agenzia2000'. We acknowledge the European Synchrotron Radiation Facility for providing the synchrotron radiation facilities and we would like to thank Dr. G. Leonard for assistance in using beamline ID14-4. We also acknowledge access to the Elettra Synchrotron (Italy) and we would like to thank the X-ray beamline staff. The authors are grateful to M. Amendola, G. Sorrentino, L. de Luca and P. Occorsio for their technical assistance.

References

[1] Esposito, L., Sica, F., Raia, C.A., Giordano, A., Rossi, M., Mazzarella, L. and Zagari, A. (2002) J. Mol. Biol. 318, 463–477.
[2] Raia, C.A., Giordano, A. and Rossi, M. (2001) Methods Enzymol. 331, 176–195.
[3] Eklund, H. and Branden, C.-I. (1987) in: Biological Macromolecules and Assemblies (Jurnak, F. and McPherson, A., Eds.), Vol. 3, pp. 73–142, Wiley/Interscience, New York.
[4] Meijers, R., Morris, R.J., Adolph, H.W., Merli, A., Lamzin, V.S. and Cedergren-Zeppezauer, E.S. (2001) J. Biol. Chem. 276, 9316–9321.
[5] Korkhin, Y., Kalb, A.J., Peretz, M., Bogin, O., Burstein, Y. and Frolow, F. (1998) J. Mol. Biol. 278, 967–981.
[6] Giordano, A., Cannio, R., La Cara, F., Bartolucci, S., Rossi, M. and Raia, C.A. (1999) Biochemistry 38, 3043–3054.
[7] Pearl, L., Demasi, D., Hemmings, A.M., Sica, F., Mazzarella, L., Raia, C.A., D'Auria, S. and Rossi, M. (1993) J. Mol. Biol. 229, 782–784.
[8] Otwinowski, Z. and Minor, W. (1997) Methods Enzymol. 276, 307–326.
[9] Navaza, J. (1994) Acta Crystallogr. A50, 157–163.
[10] Brunger, A.T. et al. (1998) Acta Crystallogr. D54, 905–921.
[11] Jones, T.A., Zou, J.Y., Cowan, S.W. and Kjeldgaard, M. (1991) Acta Crystallogr. A47, 110–119.
[12] Laskowski, R.A., MacArthur, M.W., Moss, M.D. and Thorton, J.M. (1993) J. Appl. Crystallogr. 26, 283–291.
[13] Al-Karadaghi, S., Cedergren-Zeppezauer, E.S., Hoevmoller, S., Petratos, K., Terry, H. and Wilson, K.S. (1994) Acta Crystallogr. D50, 793–807.
[14] Ramaswamy, S., Park, D.H. and Plapp, B.V. (1999) Biochemistry 38, 13951–13959.
[15] Rubach, J.K., Ramaswamy, S. and Plapp, B.V. (2001) Biochemistry 40, 12686–12694.
[16] Eklund, H., Samama, J.P. and Jones, T.A. (1984) Biochemistry 23, 5982–5996.
[17] Cedergren-Zeppezauer, E. (1983) Biochemistry 22, 5761–5772.
[18] Samama, J.P., Zeppezauer, E., Biellmann, J.F. and Branden, C.I. (1977) Eur. J. Biochem. 81, 403–409.
[19] Tsou, C.-L. (1998) Biochemistry (Moscow) 63, 253–258.
[20] Fan, Y., Ju, M., Zhou, J. and Tsou, C. (1995) Biochim. Biophys. Acta 1252, 151–157.
[21] Kraulis, P.J. (1991) J. Appl. Crystallogr. 24, 946–950.
[22] Merritt, E.A. and Bacon, D.J. (1997) Methods Enzymol. 277, 505–524.